Research Square

Preprints are preliminary reports that have not undergone peer review.
They should not be considered conclusive, used to inform clinical practice,
or referenced by the media as validated information.

Genome-wide identification and characterization of the smyd gene family in Chinese perch (Siniperca chuatsi): evolutionary divergence and spatiotemporal expression patterns during development and skeletal muscle injury response

Yaxiong Pan
Changsha University
Dezhi Wu
Changsha University
Yifan Zhu
Hunan Normal University
Shuangli He
Changsha University
Danshi Bingma
Changsha University
Jinyang Jiang
Changsha University
Linxuan Zhang
Changsha University
Zhi Luo
Huazhong Agricultural University
Xin Zhu
Changsha University
Jianshe Zhang
Changsha University
Wuying Chu
chuwuying18@163.com
Changsha University

Research Article

Keywords: smyd gene family, Siniperca chuatsi, developmental expression, skeletal muscle, muscle injury

Posted Date: November 13th, 2026

DOI: https://doi.org/10.21203/rs.3.rs-11186222/v1

License: This work is licensed under a Creative Commons Attribution 4.0 International License.
Read Full License

Additional Declarations: No competing interests reported.

Genome-wide identification and characterization of the *smyd* gene family in Chinese perch (*Siniperca chuatsi*): evolutionary divergence and spatiotemporal expression patterns during development and skeletal muscle injury response

Yaxiong Pan[1], Dezhi Wu[1], Yifan Zhu[2], Shuangli He[1], Danshi Bingma[1], Jinyang Jiang[1], Linxuan Zhang[1], Zhi Luo[3], Xin Zhu[1], Jianshe Zhang[1], Wuying Chu[1 *]

[1] *Hunan Provincial Key Laboratory of Nutrition and Quality Control of Aquatic Animals, Hunan Engineering Technology Research Center for Amphibian and Reptile Resource Protection and Product Processing, College of Biological and Chemical Engineering, Changsha University, Changsha 410022, Hunan, P.R. China.*

[2] *College of Life Sciences, Hunan Normal University, Changsha 410081, P.R. China.*

[3] *College of Fisheries, Huazhong Agricultural University, Wuhan 430070, Hubei, P.R. China.*

** Corresponding author. E-mail address: biopyx@163.com*

Abstract

The SET and MYND domain-containing (SMYD) proteins are lysine methyltransferases involved in chromatin regulation, muscle development, and cellular processes such as proliferation and differentiation. However, the genome-wide characteristics and expression patterns of the *smyd* gene family in Chinese perch (*Siniperca chuatsi*) remain unclear. In this study, seven *smyd* genes were identified in the Chinese perch genome, including *smyd1a*, *smyd1b*, *smyd2a*, *smyd2b*, *smyd3*, *smyd4*, and *smyd5*. Phylogenetic and structural analyses classified these genes into five conserved *smyd* subfamilies (*smyd1*, *smyd2*, *smyd3*, *smyd4* and *smyd5* subfamilies) and revealed a conservation–divergence pattern: *smyd1*, *smyd2*, and *smyd3* retained relatively conserved domain architectures and motif compositions, whereas *smyd4* and *smyd5* showed greater structural divergence. Expression profiling revealed clear spatiotemporal divergence between duplicated *smyd1* paralogs: *smyd1b* was relatively enriched during early embryogenesis, whereas *smyd1a* became predominant after hatching and was strongly enriched in adult skeletal muscle, especially white muscle. Following cardiotoxin-induced skeletal muscle injury, the seven *smyd* genes displayed distinct temporal responses during repair and regeneration. These findings provide a systematic basis for understanding the evolution and potential involvement of *smyd* genes in Chinese perch.

Keywords: *smyd* gene family, *Siniperca chuatsi*, developmental expression, skeletal muscle, muscle injury

1. Introduction

Protein methylation is an evolutionarily conserved post-translational modification involved in chromatin remodeling, transcriptional regulation, and diverse cellular processes such as proliferation, differentiation, and survival (Rueda-Robles et al. 2021; Padilla et al. 2023). Lysine methyltransferases are key enzymes mediating this modification, catalyzing the transfer of methyl groups to lysine residues in histone and non-histone substrates. Through this modification, lysine methyltransferases can influence substrate protein stability, localization, protein–protein interactions, and enzymatic activity. The *smyd* family represents a distinct subgroup of lysine methyltransferases characterized by the presence of SET and MYND domain-related structural features. In most SMYD proteins, the catalytic SET domain is interrupted by a MYND zinc-finger domain, giving rise to the name SMYD, which refers to SET and

MYND domain-containing proteins (Li and Zhang 2009; Du et al. 2014; Rueda-Robles et al. 2021). The *smyd1/Bop* gene was first described in mice (Hwang and Gottlieb 1995; Hwang and Gottlieb 1997). Subsequent studies have shown that SMYD proteins participate in chromatin regulation, transcriptional control, and diverse cellular processes (Rueda-Robles et al. 2021; Padilla et al. 2023). Although *smyd* members share conserved structural features, different family members have undergone functional diversification during evolution.

Five *smyd* members (*smyd1-smyd5*) have been identified in mammals, and accumulating evidence indicates that each member has acquired specialized biological functions (Han et al. 2024). *The smyd1* is a muscle-enriched lysine methyltransferase with essential roles in skeletal and cardiac muscle development (Tan et al. 2006; Nagandla et al. 2016). In zebrafish, *smyd1* is required for sarcomere organization and normal muscle function (Jiao et al. 2021; Diofano et al. 2025). *The smyd2* has also been implicated in skeletal muscle development and myofilament organization (Donlin et al. 2012). Although *smyd2* and *smyd3* are more widely known for their roles in tumor cell proliferation, tumorigenesis, and metastasis (Mazur et al. 2014; Bottino et al. 2020; Wu et al. 2021a), *smyd3* has also been reported to promote myogenesis by activating the myogenin regulatory network (Codato et al. 2019). Recently, *smyd3* in Chinese perch was reported to negatively regulate antiviral immunity, indicating that *smyd* members may also participate in immune-related or stress-related biological processes (Shi et al. 2026). In addition, *smyd4* is required for cardiac development in zebrafish (Xiao et al. 2018), while *smyd5* plays important roles in hematopoiesis during zebrafish embryogenesis and in the regulation of heterochromatin and chromosome integrity during embryonic stem cell differentiation (Fujii et al. 2016; Kidder et al. 2017). Teleost fish have experienced a teleost-specific whole-genome duplication (TS-WGD), which contributed to the retention of duplicated paralogs for many genes (Glasauer and Neuhauss 2014). In zebrafish, duplication events have given rise to paralogous copies of *smyd1* and *smyd2*, designated as *smyd1a*, *smyd1b*, *smyd2a*, and *smyd2b*. Both *smyd1a* and *smyd1b* are involved in skeletal and cardiac muscle development, but *smyd1b* appears to play a more prominent role during embryonic stages (Gao et al. 2014; Wang et al. 2016). These findings suggest that duplicated *smyd* genes may undergo functional divergence during teleost evolution.

Skeletal muscle is one of the most abundant tissues in vertebrates, typically accounting for approximately 40–60% of body mass in adult fishes. It serves as the primary effector of the locomotor system and a major site for energy utilization and metabolic regulation, and exhibits remarkable plasticity in response to developmental cues, mechanical loading, and injury (Nemova et al. 2021; Rossi and Borowiec 2024). In teleost fishes, muscle growth proceeds in two complementary modes, hyperplasia and hypertrophy, and continues throughout life, in contrast to the largely determinate growth pattern of mammals (Johnston et al. 2011). Following acute damage, the regenerative response of skeletal muscle is driven by Pax7-positive satellite cells that activate, proliferate, differentiate, and fuse to form new myofibers, a program tightly orchestrated by the myogenic regulatory factors (MyoD, Myf5, MYOG, MRF4) and by epigenetic machinery acting at their loci (Hardy et al. 2016; Wang et al. 2022). Cardiotoxin (CTX) can induce synchronous and reproducible muscle injury while sparing the vasculature, satellite-cell niche, and innervation, making it one of the most widely used models for dissecting the molecular dynamics of muscle repair (Hardy et al. 2016; Wang et al. 2022). However, despite increasing evidence that lysine methyltransferases—including *smyd1*, *smyd3*, and *smyd5* have been implicated in developmental or epigenetic programs related to myogenesis and stem-cell regulation and may govern stem-cell behavior, the participation of the *smyd* family in adult skeletal-muscle regeneration in vivo, particularly in teleosts, remains poorly defined.

Chinese perch (*Siniperca chuatsi*) is one of the most commercially important freshwater carnivorous fish species in China and is valued for its high-quality flesh, rich essential amino acid content, and abundant unsaturated fatty acids (Chu et al. 2010). As an ambush predator, Chinese perch relies on rapid locomotor responses during prey capture, and white muscle, which is mainly composed of fast-twitch fibers, plays an important role in burst swimming. Our previous studies suggested that the miRNA–*smyd1* regulatory network may participate in the development and functional specialization of different muscle fiber types in Chinese perch and provided molecular characterization and expression profiles of *smyd1a* and *smyd1b* (Wang et al. 2016; Chu et al. 2017). However, our understanding of the *smyd* gene family in Chinese perch remains fragmented. Although teleost-specific whole-genome duplication has generated duplicated *smyd* paralogs in many fish species, it remains unclear whether these paralogs have retained conserved protein structures while undergoing divergent developmental and tissue-expression patterns in Chinese perch. Despite the known involvement of several SMYD proteins in myogenesis and muscle function, whether *smyd* family members respond to adult skeletal muscle injury and repair in teleosts remains poorly understood. To address these gaps, the present study performed a comprehensive genome-wide identification and characterization of the *smyd* gene family in Chinese perch. The identified *smyd* genes were analyzed for phylogenetic relationships, conserved motif composition, domain architecture, chromosomal localization, comparative synteny, and predicted tertiary structures. Their expression profiles were further examined across adult tissues, embryonic and early larval stages, and post-hatching skeletal muscle growth. In addition, dynamic expression changes of *smyd* genes were analyzed in a cardiotoxin-induced muscle injury model to explore their potential involvement in skeletal muscle injury response and repair.

2. Materials and methods

2.1. Identification of the *smyd* gene family

SMYD protein sequences from human and zebrafish were retrieved from NCBI and used as queries to identify candidate *smyd* genes in the Chinese perch genome database. BLASTp searches were performed using the NCBI BLAST+ program with an E-value threshold of 0.05, word size of 5, BLOSUM62 substitution matrix, gap opening cost of 11, and gap extension cost of 1. Candidate sequences were manually checked to remove redundant or incomplete hits. The conserved domains of the candidate proteins were then examined using conserved domain annotation tools, including the NCBI Conserved Domain Database, to confirm their identity as members of the *smyd* family. Candidates were retained based on sequence similarity to known SMYD proteins and the presence of characteristic *smyd*-related domains, particularly the SET domain and/or MYND-associated domain architecture. Finally, seven *smyd* genes were identified in *Siniperca chuatsi*.

2.2. Physicochemical properties analysis

The amino acid length, molecular weight (MW), and theoretical isoelectric point (pI) of each Chinese perch SMYD protein were calculated using TBtools v2.481 (Chen et al. 2020). The exon number of each *smyd* gene was determined from the genome annotation file and summarized using TBtools.

2.3. Phylogenetic analysis

To investigate the evolutionary relationships of the *smyd* gene family in Chinese perch, *smyd* sequences were retrieved from the genomes of zebrafish (*Danio rerio*), Atlantic salmon (*Salmo salar*), Chinese medaka (*Oryzias sinensis*), Nile tilapia (*Oreochromis niloticus*), common carp (*Cyprinus carpio*), denticle herring (*Denticeps clupeoides*), electric eel (*Electrophorus electricus*), large yellow croaker (*Larimichthys crocea*), human (*Homo sapiens*), and mouse (*Mus musculus*) using the NCBI (http://www.ncbi.nlm.nih.gov/) and Ensembl (https://www.ensembl.org/) databases. Multiple sequence

alignment of SMYD amino acid sequences was performed in MEGA 11.0 with MUSCLE under default settings (Tamura et al. 2021). Cross-species phylogenetic analysis was conducted using MEGA 11.0 to construct a Neighbor-joining tree, with the Jones-Taylor-Thornton (JTT) model and branch support was assessed using 1,000 bootstrap replicates. The resulting phylogenetic tree was visualized and annotated using iTOL (Letunic and Bork 2021).

2.4. Gene structure and chromosomal localization analysis

Conserved motifs in SMYD protein sequences were identified using the web-based MEME Suite 5.5.8 (https://meme-suite.org/meme/tools/meme), with the following parameters: maximum number of motifs = 10, motif width = 6-50 amino acids, and E-value threshold = 1e-5 (Bailey et al. 2015). Conserved domains were annotated using the NCBI Conserved Domain Database (CDD), with an expect value cutoff of 0.01 and a maximum number of hits of 500. The conserved motif distributions and domain architectures were visualized using Chiplot (https://www.chiplot.online/) (Xie et al. 2023). Genomic coordinates of *smyd* genes were extracted from the corresponding GFF3 annotation file of Chinese perch, and chromosomal localization maps were generated using TBtools.

2.5. Comparative synteny analysis of *smyd* genes

Comparative synteny analysis was performed to investigate the conservation of *smyd* genomic loci among Chinese perch, large yellow croaker, and zebrafish. Genome annotation files and predicted protein sequences of the three species were used for pairwise genome collinearity analysis. All-against-all BLASTP searches were first conducted using predicted protein sequences, and genome-wide collinear blocks were then identified using the MCScanX module implemented in TBtools with default parameters. The chromosomal positions of *smyd* genes were extracted from the corresponding genome annotation files. Syntenic blocks containing *smyd* genes were selected and visualized using TBtools.

2.6. Protein tertiary structure prediction and visualization

The complete amino acid sequences of the seven Chinese perch SMYD proteins were submitted to AlphaFold 3 for tertiary structure prediction. Model confidence was evaluated using the predicted TM-score (pTM) and ranking score provided by AlphaFold 3 (Abramson et al. 2024). Predicted models with pTM values ≥ 0.80 were considered high-confidence models. For each SMYD protein, the model with the highest AlphaFold 3 ranking score among the high-confidence predictions was selected for subsequent visualization and structural comparison. The selected structures were visualized using PyMOL v1.7.2.1 in cartoon representation (Schrödinger 2015).

2.7. Tissue specificity and developmental expression analysis of *smyd* genes

To characterize the expression profiles of Chinese perch *smyd* genes in different tissues and developmental stages, transcriptome sequencing data from 17 adult tissues, including liver, spleen, gallbladder, skin, esophagus, stomach, gastric cecum, intestine, testis, ovary, gill, pseudobranch, muscle, head kidney, posterior kidney, myocardium, and brain, and 9 developmental stages, including 2-cell embryo, 1k-cell embryo, blastocyst, gastrula, pigment period, tail-bud, before out from membrane, 1 day post-hatching, and 5 days post-hatching, were obtained from the NCBI SRA database under BioProject accession PRJNA496427, as contributed by Shen (Shen et al. 2020). Additionally, the transcriptomic datasets for white and red skeletal muscles were obtained from our previous study (BioProject accession PRJNA685101) (Wu et al. 2021b). The transcriptome data were analyzed according to the protocols described in our previous study (Chen et al. 2023). The *Siniperca chuatsi* genome database was obtained from the Chinese perch genome portal (http://genomes.igb-berlin.de/Siniperca/) (He et al. 2020). The corresponding genome annotation files, coding sequences, and protein sequences were used for gene identification and subsequent comparative analyses.

2.8. Muscle injury in Chinese perch

The methodology for establishing the cardiotoxin (CTX)-induced skeletal muscle injury model in Chinese perch was adapted from our previous study (Meng et al. 2025). Briefly, Chinese perch (5.85 ± 0.82 g) were subjected to an intramuscular injection of 40 μL of CTX (10 μmol/L) into the dorsal white muscle to induce injury. Sampling was performed at four time points post-injury: 1, 3, 5, and 7 days post-injury (dpi), the uninjured control group was designated as 0 dpi for comparison, with six fish collected per time point. At each time point, white muscle surrounding the injection site was collected. A portion of the tissue was fixed for histological examination, whereas the remaining tissue was immediately snap-frozen in liquid nitrogen and stored at −80 °C for RNA extraction.

2.9. Histological examination of skeletal muscle injury in Chinese perch

To histologically verify CTX-induced skeletal muscle injury, muscle samples encompassing the injection site were collected. Samples were fixed in Eco-friendly GD Muscle Fixative Solution (Servicebio, Wuhan, China, G1111), paraffin-embedded, sectioned at 4 μm. Sections were stained with hematoxylin and eosin (H&E) and examined under a light microscope. Representative images were acquired from the injured region using identical imaging settings.

2.10. Quantitative PCR analysis

Total RNA was extracted using a total RNA Isolation Reagent (Biosharp, Beijing, China, BS258A). Total RNA was reverse-transcribed into cDNA using the TRUEscript RT MasterMix for qPCR (Aidlab, Beijing, China, PC7002). qPCR was performed to examine the expression of *smyd* genes in Chinese perch after muscle injury. Gene-specific qPCR primers were designed by Primer Premier 5.0 (Table 1). ef1α and rpl13a were selected as internal reference genes. qPCR was carried out on VQ-100B instrument (YUANZAN, Shanghai, China) using MagicSYBR Mixture (cwbio, Shanghai, China, CW3008M). The PCR program was as follows: 95°C for 1 min; 40 cycles of 95°C for 5 s, 60°C for 30 s; followed by a melting curve from 65°C to 95°C in 0.5°C increments. Relative expression levels were calculated using the $2^{-\Delta\Delta CT}$ method.Each qPCR reaction was performed in technical triplicate for each biological sample. Six fish were collected at each time point and each fish was treated as an independent biological replicate (n = 6 per time point). The specificity of each primer pair was confirmed by melting-curve analysis showing a single amplification peak. Primer amplification efficiency was evaluated using serially diluted cDNA, and only primer pairs with acceptable amplification efficiency were used for subsequent analysis. The Ct values of target genes were normalized against the geometric mean of two reference genes, ef1α and rpl13a. Relative expression levels were calculated using the $2^{-\Delta\Delta CT}$ method, with the 0 dpi group used as the calibrator. Data are presented as the mean ± SEM. Differences among time points were analyzed by one-way ANOVA followed by Tukey's multiple comparisons test. Statistical significance was defined as $P < 0.05$. Different lowercase letters indicate significant differences among groups.

Table 1 The qPCR primer sequences

Gene Name	Forward Primer Sequence (5′–3′)	Reverse Primer Sequence (5′–3′)
ef1α	GCGTCAGCGGCTTCCTCAA	TCCCTTCGTCTGGCTTTCC
rpl13a	GCGTCTTTCTTTTCGCACAT	GCCTTCACATCTCACCACCA
smyd1a	TTTGGCTGTAGCAGGGTTC	GCCGAGGGATAAGGGACTA
smyd1b	TGTGGAGCACATTAAGTGAGG	AGAGCAGCATTGTTTGGGT
smyd2a	GAAGGAGCTATGAGCTACGGA	CCAGCCCCAAATACAGACG
smyd2b	TGCCCGACCATAAAGACCT	TGACTATGACGCTGGGAAGA
smyd3	GAGAACCCCTCAGCCTTATT	ACAGTTTGGCCTACAGTCATG
smyd4	ACAGCCGATACTGCTCAACTT	AACCCCGCCTTTAGTGTTAC

smyd5	CTTCCTTATCGCACTGACTGA	CGAAAACCACCTGAGAACC

3. Results

3.1. Characteristics of *smyd* genes in Chinese perch

Seven *smyd* gene family members were identified in the Chinese perch genome and named *smyd1a*, *smyd1b*, *smyd2a*, *smyd2b*, *smyd3*, *smyd4*, and *smyd5* based on phylogenetic analysis. Their physicochemical properties and genomic features are summarized in Table 2. The protein lengths and exon numbers of *smyd* genes in Chinese perch were relatively conserved. Except for *smyd4*, all *smyd* genes were found to consist of 10–14 exons, encoding proteins of 440–489 amino acids. *Smyd4* encoded a much longer protein of 786 amino acids. The molecular weights of the encoded proteins ranged from 50 to 87 kDa. The isoelectric points of most *smyd* proteins were acidic, ranging from 5.07 to 6.89, with the exception of *smyd1a* (pI = 7.32) and *smyd2b* (pI = 8.48), which were predicted to be neutral and basic, respectively.

Table 2 Characteristics of the *smyd* gene family in Chinese perch

Gene	Chr ID	Protein length (aa)	Number of exons	Molecular weight (Da)	Isoelectric point	Gene id
smyd1a	Chr13	479	10	54248.24	7.32	SC7-LG13_16943
smyd1b	Chr07	489	10	56259.43	6.2	SC7-LG07_09102
smyd2a	Chr16	444	12	51066.55	5.9	SC7-LG16_20201
smyd2b	Chr12	463	12	53021.29	8.48	SC7-LG12_16230
smyd3	Chr16	443	12	50716.13	6.08	SC7-LG16_20184
smyd4	Chr22	786	10	87167.86	6.89	SC7-LG22_28309
smyd5	Chr21	440	14	50063.71	5.07	SC7-LG21_26677

3.2. Functional domain and conserved motif analysis of *smyd* genes in Chinese perch

To investigate the structural characteristics of *smyd* family proteins in Chinese perch, the conserved motifs and functional domains of seven SMYD proteins were predicted. Conserved motifs and functional domains were predicted using MEME and the NCBI Conserved Domain Database (CDD), respectively. (Fig. 1A). Conserved domain analysis revealed that all seven *smyd* family members in Chinese perch possess the SET domain, consistent with the conserved features of the *smyd* family identified in other species. Except for *smyd5*, the remaining six members concurrently contain the zf-MYND zinc-finger domain. In *smyd1a*, *smyd1b*, *smyd2a*, *smyd2b*, and *smyd3*, the zf-MYND domain is embedded within the SET domain. In contrast, the zf-MYND domain of *smyd4* is located at the N-terminus of the SET domain, displaying a different structural arrangement compared to the aforementioned isoforms. Notably, *smyd5* contains only the SET domain and lacks the zf-MYND domain. Conserved motif analysis identified a total of 10 conserved motifs. *The smyd1a*, *smyd1b*, *smyd2a*, *smyd2b*, and *smyd3* share most of the same motifs (motif 1–motif 9) with a highly similar sequential arrangement, implying that these genes are highly conserved in terms of function and evolutionary relationship, which is consistent with the CDD domain analysis. Furthermore, compared to other isoforms, *smyd1a* and *smyd1b* additionally contain motif 10, implying a degree of structural specificity in these two subtypes. In contrast, the motif compositions of *smyd4* and *smyd5* deviate substantially from those of other family members, as both lack several motifs that are otherwise highly conserved. In addition, marked differences in motif composition and arrangement are observed between *smyd4* and *smyd5*, further suggesting that these two members may have undergone functional specialization. The seven *smyd* genes were distributed across six chromosomes, with *smyd2a* and *smyd3* both located on Chr16 (Fig. 1B).

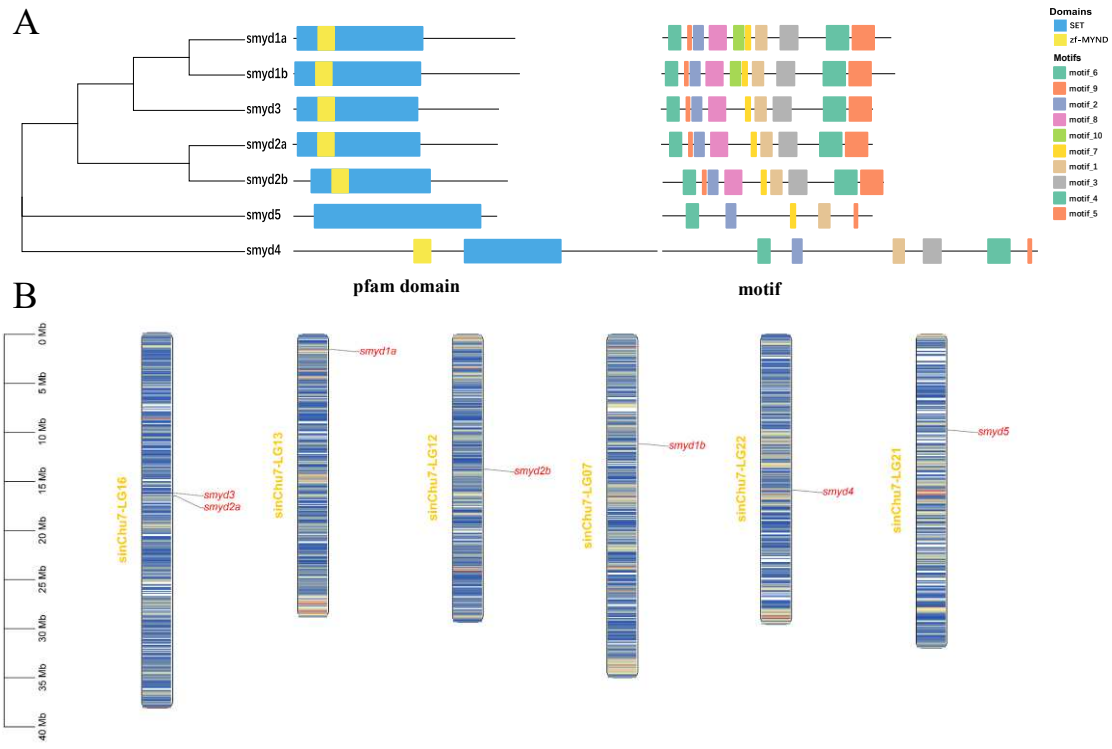


Fig. 1 Functional domain and chromosomal localization of the *smyd* gene family in Chinese perch. (A) Functional domain of the *smyd* gene family in Chinese perch. The phylogenetic tree was constructed using MEGA11 by the neighbor-joining method with 1,000 bootstrap replicates, based on amino acid sequence alignment. (B) Chromosomal localization of the *smyd* gene family in Chinese perch.

3.3. Comparative synteny analysis of *smyd* genes in teleosts

To examine the genomic context of *smyd* genes across teleost species, comparative synteny analysis was performed among Chinese perch, large yellow croaker, and zebrafish (Fig. 2). Genome-wide collinear blocks were observed among the three genomes, as shown by the gray connecting lines. Several *smyd*-associated collinear relationships were detected and are highlighted by blue lines. Between Chinese perch and large yellow croaker, which are both percomorph teleosts, all seven Chinese perch *smyd* genes showed syntenic relationships with their corresponding *smyd* loci in large yellow croaker. Among them, the region containing *smyd2a* and *smyd3* in Chinese perch corresponded to a *smyd2a/smyd3*-containing region in large yellow croaker. In contrast, the *smyd*-associated collinear links between Chinese perch and zebrafish were distributed across more linkage groups.

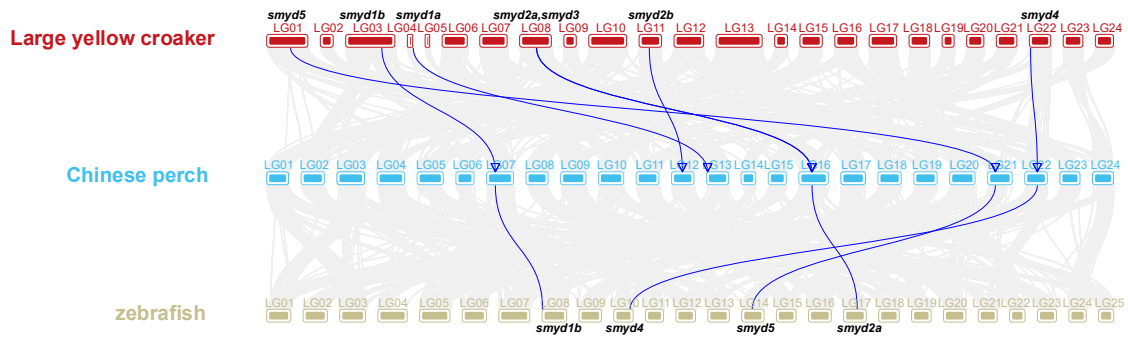


Fig. 2 Chromosomes or linkage groups of large yellow croaker, Chinese perch, and zebrafish are shown in red, blue, and khaki, respectively. Gray curves represent genome-wide collinear blocks between species, whereas blue curves highlight syntenic relationships involving *smyd* genes. The positions of

smyd genes are indicated beside the corresponding linkage groups.

3.4. Prediction and comparison of tertiary structures of SMYD proteins

To further compare the structural characteristics of Chinese perch SMYD proteins, tertiary structures of the seven SMYD members were predicted using AlphaFold 3 and visualized with PyMOL. The predicted structures of all SMYD proteins contained prominent α-helices and β-strands, together with variable disordered loop regions (Fig. 3). SMYD1a and SMYD1b displayed highly similar overall folds, and a comparable structural resemblance was also observed between SMYD2a and SMYD2b, consistent with their close phylogenetic relationships and conserved domain/motif compositions. SMYD3 shared a compact α/β fold similar to those of SMYD1 and SMYD2 members. In contrast, SMYD4 exhibited a more distinct and extended predicted structure, which may be associated with its longer protein sequence and different domain arrangement. SMYD5 also retained a compact predicted fold but showed structural differences from SMYD1–SMYD3. Overall, the predicted tertiary structures support the conservation of SMYD1, SMYD2, and SMYD3 members and the greater structural divergence of SMYD4 and SMYD5, suggesting possible functional differentiation among Chinese perch SMYD proteins.

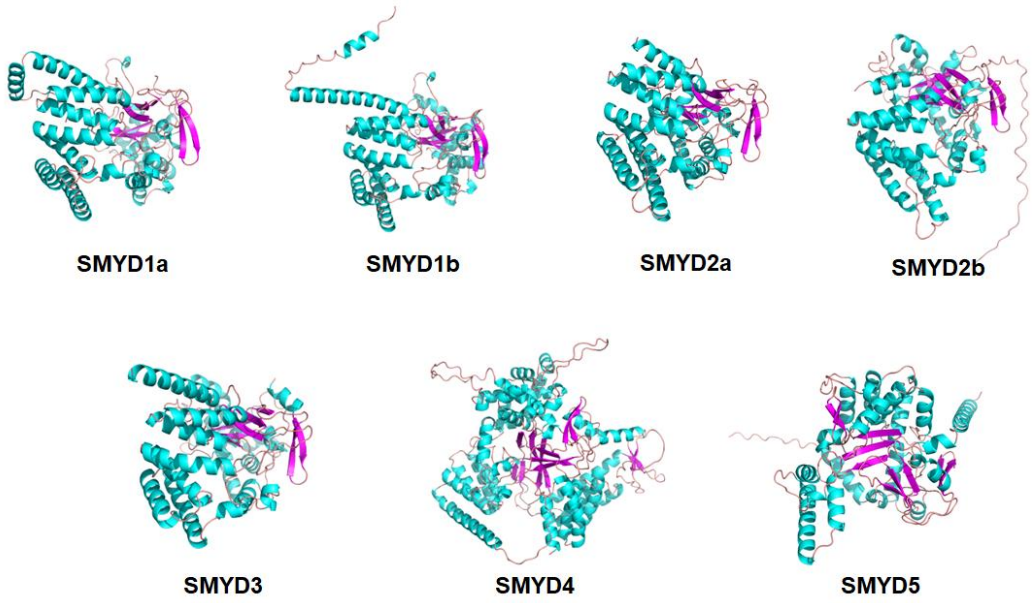


Fig. 3 Predicted 3D structure of Chinese perch SMYD proteins, annotated with α-helices (cyan), β-strands (magenta), and disordered regions (pink).

3.5. Phylogenetic analysis of the *smyd* gene family

To investigate the phylogenetic relationships of the *smyd* gene family in Chinese perch, full-length SMYD protein sequences from Chinese perch and representative vertebrate species were aligned to construct a Neighbor-joining phylogenetic tree. The tree topology clearly divided the *smyd* genes into five major clades, corresponding to the *smyd1, smyd2, smyd3, smyd4,* and *smyd5* subfamilies, with Chinese perch *smyd* genes distributed across all five clades (Fig. 4). Within the *smyd1* clade, mammals possess a single *smyd1* ortholog, whereas teleost fishes harbor two paralogous subtypes, *smyd1a* and *smyd1b*. The tree topology showed that all teleost *smyd1a* sequences formed a well-supported fish-specific *smyd1a* subclade, and all teleost *smyd1b* sequences formed a separate *smyd1b* subclade. These two fish-specific subclades then grouped together to form a unified teleost *smyd1* clade, which in turn clustered with the mammalian *smyd1* sequences to constitute the overall *smyd1* clade. This topology is

consistent with the pattern of gene duplication driven by the teleost-specific whole-genome duplication (TS-WGD), indicating that the additional *smyd1* paralog in Chinese perch originated from this duplication event. A similar topological pattern was observed within the *smyd2* clade, where teleost *smyd2a* and *smyd2b* sequences each formed distinct fish-specific subclades, suggesting that the *smyd2* paralogs in Chinese perch also likely arose through the TS-WGD, consistent with the pattern observed for *smyd1*. Notably, the *smyd1, smyd2*, and *smyd3* clades formed a well-supported monophyletic group within the phylogenetic tree, whereas the *smyd4* and *smyd5* clades were positioned outside this assemblage, indicating that *smyd1, smyd2,* and *smyd3* are more closely related to one another than to *smyd4* and *smyd5*. This phylogenetic clustering is consistent with the findings from the conserved domain and motif analyses, in which *smyd1a, smyd1b, smyd2a, smyd2b,* and *smyd3* shared highly similar domain architectures and motif compositions, whereas *smyd4* and *smyd5* exhibited substantially divergent structural features. Together, these results suggest that *smyd1, smyd2,* and *smyd3* members may share more similar biological functions, while *smyd4* and *smyd5* have likely undergone greater functional divergence during evolution.

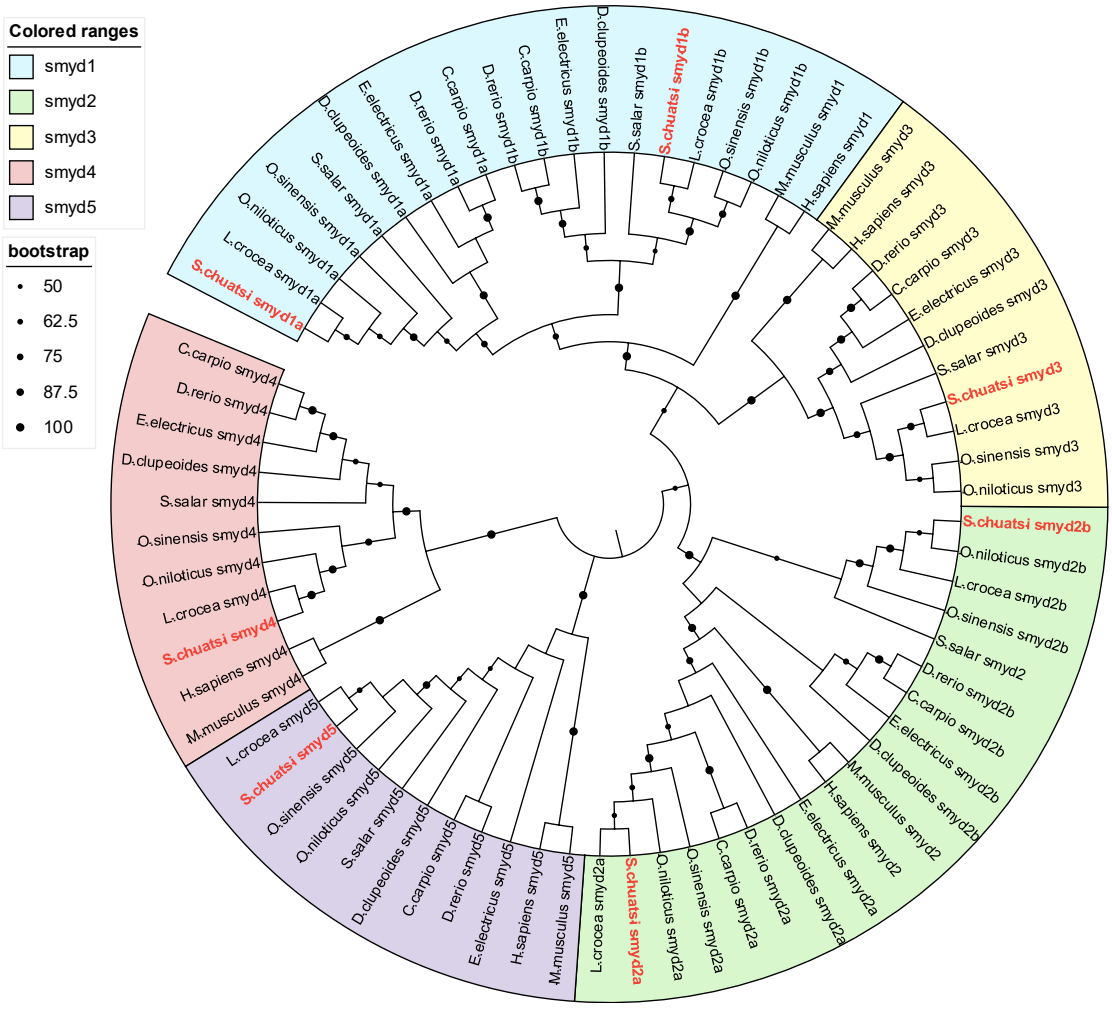


Fig. 4 Phylogenetic tree of *smyd* genes of different species. The seven *Siniperca chuatsi smyd* genes are highlighted in bold red font. The diameter of circles on the branch represents a percentage of 1000 bootstrap replicates

3.6. Developmental expression patterns of *smyd* genes during embryonic and early larval stages

To investigate the developmental expression dynamics of the *smyd* gene family during early

ontogeny, transcriptomic data from nine developmental stages, including the 2-cell embryo, 1k-cell embryo, blastocyst, gastrula, pigment period, tail-bud stage, before out from membrane, 1 day post-hatching, and 5 days post-hatching, were analyzed in Chinese perch (Fig. 5). The seven *smyd* genes displayed distinct temporal expression patterns during embryonic and early larval development. *smyd*1a showed very low expression during early embryonic stages and became detectable from the tail-bud stage onward. Its expression increased during subsequent developmental stages. By contrast, *smyd*1b was detected at the 2-cell stage, decreased at the 1k-cell stage, and then increased again from the blastocyst stage, maintaining relatively high expression during later embryonic and early post-hatching stages. The two *smyd2* paralogs showed different expression patterns. *The smyd2a* exhibited relatively high expression during early embryonic stages, particularly at the 2-cell stage, and maintained detectable expression throughout the examined stages. In contrast, *smyd2b* showed low expression during early embryogenesis and increased from the tail-bud stage onward. *The smyd3* remained at relatively low expression levels across most developmental stages. *The smyd4* showed low-to-moderate expression without a pronounced stage-specific peak. *The smyd5* was highly expressed during early embryonic stages and gradually decreased during subsequent development. Overall, *smyd1b*, *smyd2a*, and *smyd5* showed relatively high expression during early embryogenesis, whereas *smyd1a* and *smyd2b* became more evident from the tail-bud stage onward.

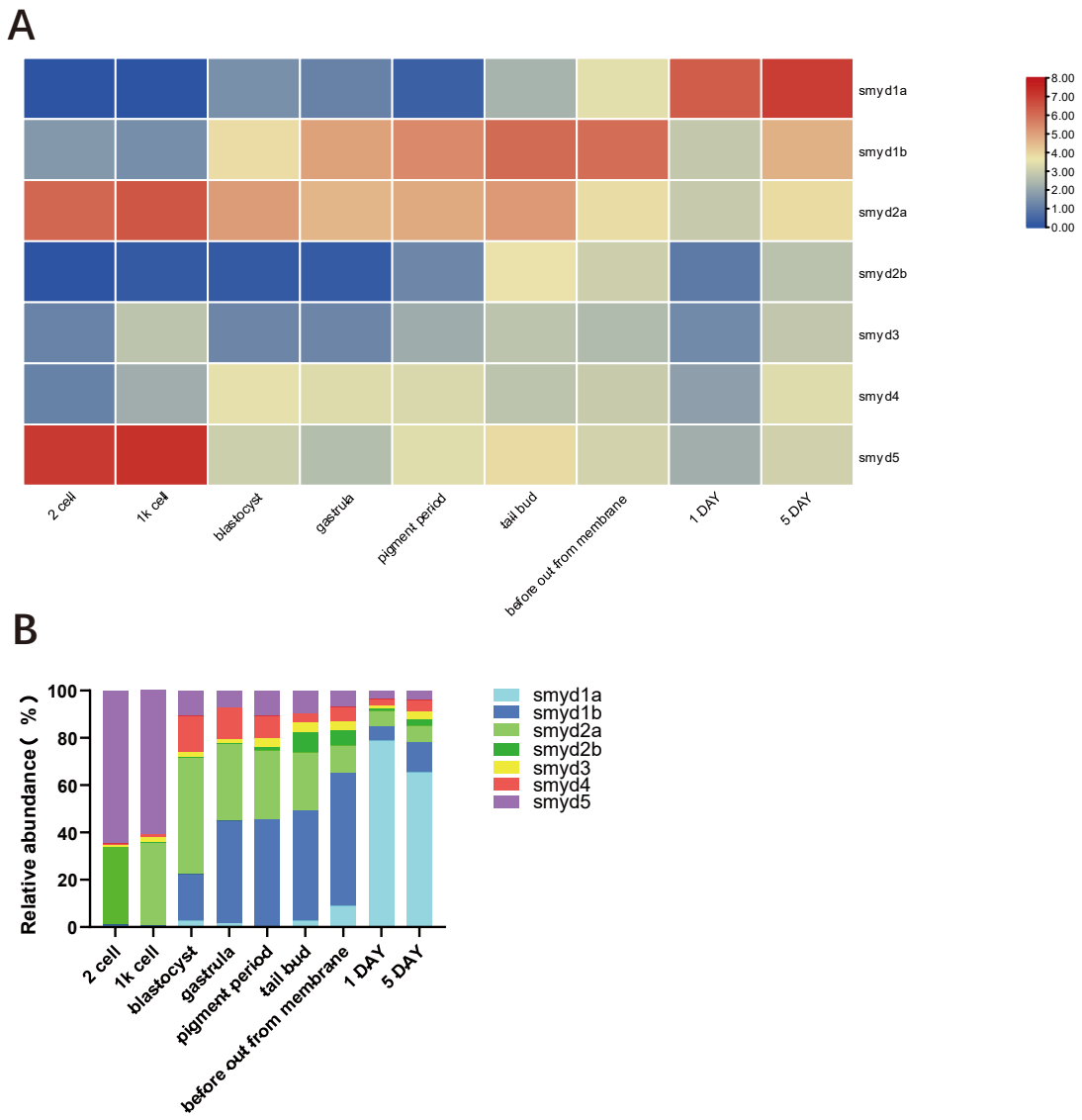


Fig. 5 Expression profiles of *smyd* genes in different developmental stages of Chinese perch. (A) Heatmap of the expression profiles of *smyd* genes in embryonic and early larval stages of Chinese perch. Red squares represent high expression level and blue squares represent low expression level of *smyd* genes. (B) Relative abundance of each *smyd* subtype in embryonic and early larval stages of Chinese perch.

3.7. Post-embryonic muscle expression patterns of *smyd* genes

To further examine *smyd* expression in muscle after hatching, transcript abundance was analyzed in skeletal muscle samples collected at 7, 15, 30, 45, 60, and 180 days post-hatching in Chinese perch (Fig. 6). Among the seven *smyd* members, *smyd1a* was the most abundant transcript at all examined stages. Its expression increased from 7 to 45 days post-hatching and remained at relatively high levels at 60 and 180 days post-hatching. *The smyd1b* was also detected throughout the post-embryonic muscle stages, but its expression level was much lower than *smyd1a*. Several *smyd* genes displayed stage-dependent changes during post-embryonic muscle growth. *The smyd2a* showed relatively higher expression at 15 days post-hatching and decreased thereafter. *The smyd2b* was also elevated at 15 days post-hatching and showed another increase at 180 days post-hatching. *smyd*4 showed relatively higher expression at 7, 60, and 180 days post-hatching, whereas *smyd5* was relatively abundant at 7 days post-hatching, decreased

during the intermediate stages, and increased again at 180 days post-hatching. In contrast, *smyd3* remained at low expression levels across all post-embryonic muscle stages. Overall, *smyd1a* represented the dominant *smyd* member during post-embryonic skeletal muscle growth, while the other *smyd* genes showed relatively lower and stage-dependent expression patterns.

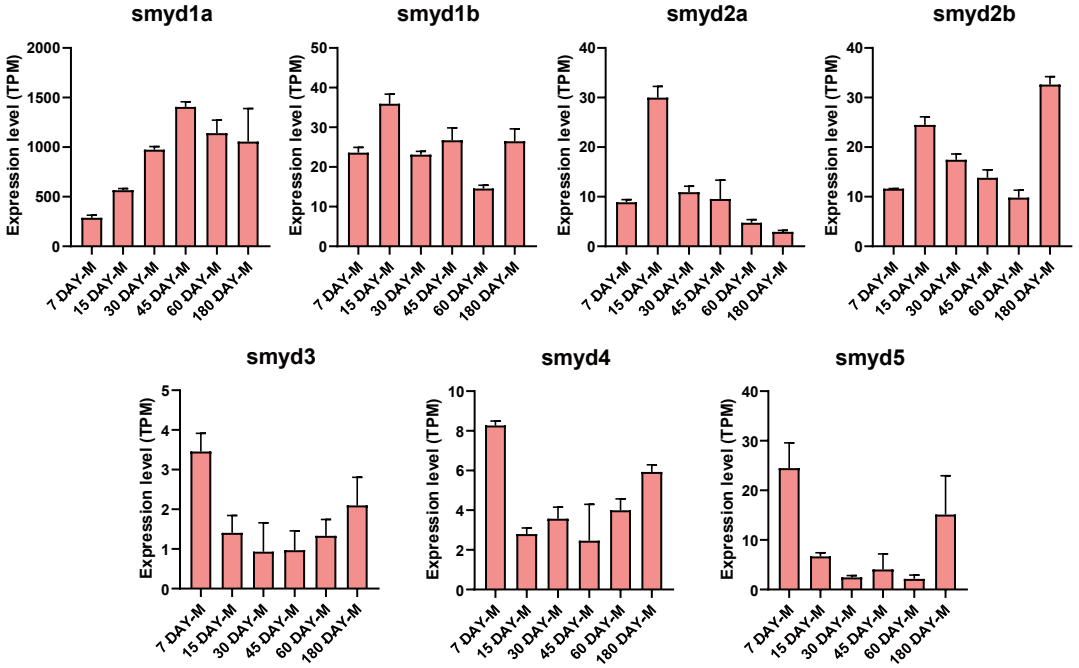


Fig. 6 Expression patterns of *smyd* genes in skeletal muscle during post-embryonic growth of Chinese perch. Expression levels of seven *smyd* genes were analyzed in skeletal muscle samples collected at 7, 15, 30, 45, 60, and 180 days post-hatching. Data are shown as mean ± SEM. The y-axis represents transcript abundance.

3.8. Tissue expression patterns of *smyd* gene family

To characterize the tissue-expression profiles of *smyd* family members, transcript abundance was examined across 17 tissues in adult Chinese perch (Fig. 7). The *smyd* genes exhibited distinct tissue-biased expression patterns. *The smyd1a* was most highly expressed in skeletal muscle, with moderate expression detected in tissues that are rich in smooth or striated muscle such as myocardium, esophagus, and intestine and relatively low expression in other tissues examined. This muscle-enriched expression pattern indicates that *smyd1a* is a muscle-preferential paralog in adult Chinese perch. *The smyd1b* showed the highest expression in the ovary and moderate expression in the brain, indicating functional divergence between *smyd1a* and *smyd1b*. Nevertheless, *smyd1b* also maintained moderate expression in skeletal muscle, myocardium, esophagus, and intestine, suggesting that it has retained partial functional overlap with *smyd1a* in muscle tissues. The tissue expression profile of *smyd2b* resembled that of *smyd1a*, with preferential expression in skeletal muscle, myocardium, esophagus, and intestine. In contrast, *smyd2a* was expressed at very low levels in muscle tissues but showed broadly moderate expression across most other tissues examined. The expression profile of *smyd3* was highly similar to that of *smyd2a*, with widespread expression across non-muscle tissues, suggesting that its functional roles may overlap with those of *smyd2a*. *The smyd4* and *smyd5* were broadly expressed across multiple tissues, including testis and ovary. Relative abundance analysis further revealed tissue-dependent differences in the contribution of individual *smyd* members to total *smyd* transcripts. In skeletal muscle, *smyd1a* was the predominant *smyd* paralog, accounting for over 95% of total *smyd* expression. In the myocardium, multiple *smyd*

members — including *smyd1a, smyd1b, smyd2b, smyd4,* and *smyd5* — contributed to total *smyd* transcripts, reflecting a more diverse expression composition in cardiac tissue. In most other tissues, with the exception of skeletal muscle and esophagus, *smyd5* constituted the dominant *smyd* paralog, suggesting a broad regulatory role for *smyd5* outside of muscle-related tissues.

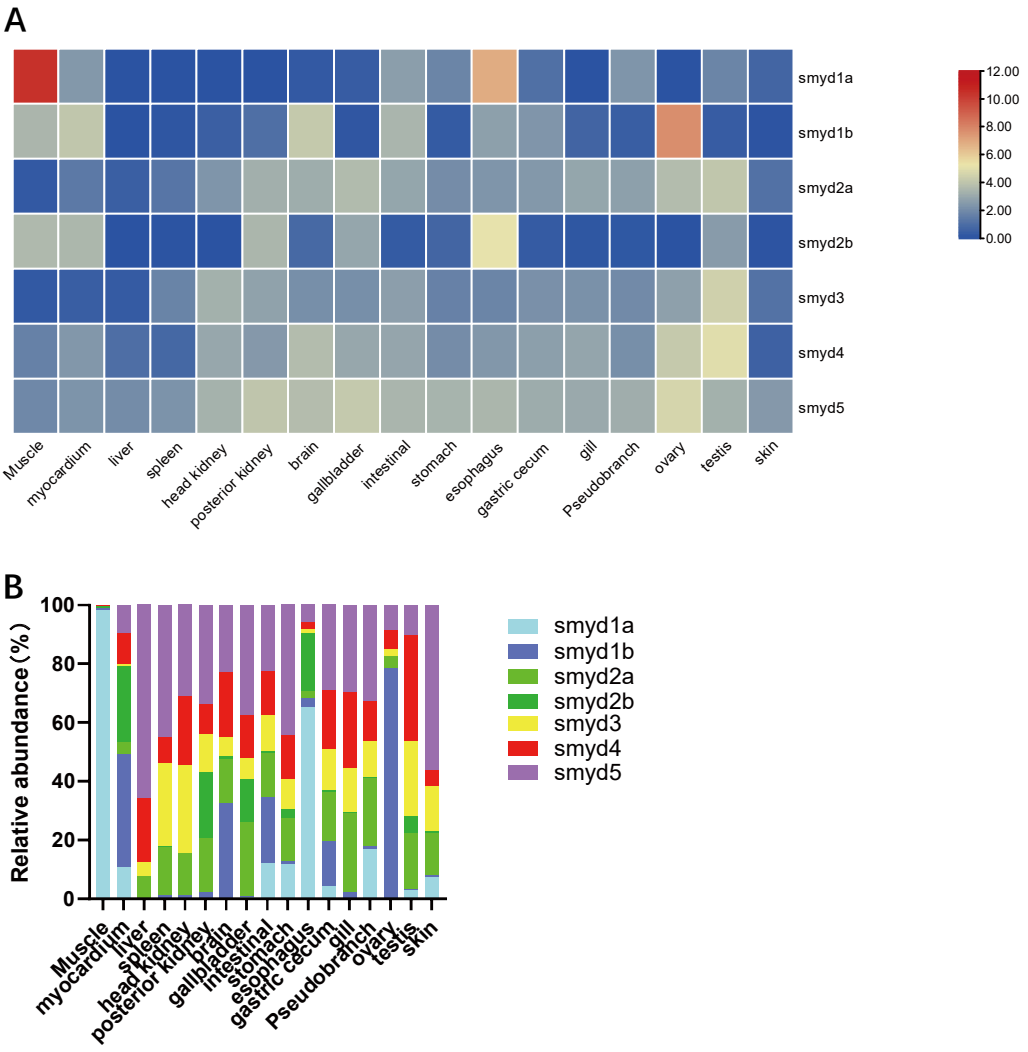


Fig. 7 Expression profiles of *smyd* genes in different tissues of Chinese perch. (A) Heatmap of the *smyd* genes expression profiles in different tissues of Chinese perch. Red squares represent high expression level and blue squares represent low expression level of *smyd* genes. (B) Relative abundance of each *smyd* subtypes expression in different tissues of Chinese perch.

3.9. Comparison of *smyd* expression of white and red muscle in Chinese perch

In teleost fish, red muscle and white muscle are spatially segregated into distinct anatomical regions, unlike the fiber-type intermingling observed in mammalian skeletal muscle. Red muscle, located in a superficial lateral strip along the body axis, is oxidative in nature, rich in mitochondria and myoglobin, and primarily supports sustained, slow-speed locomotion. White muscle, which constitutes the bulk of the body musculature, is predominantly glycolytic, composed mainly of fast-twitch fibers, and is responsible for rapid, burst-type movements. To examine the differential expression of *smyd* genes between these two functionally distinct muscle types, red and white muscle were dissected separately

from Chinese perch, and their transcriptomic profiles were analyzed by RNA sequencing (Fig. 8). The *smyd* gene family was highly expressed in both red and white muscle. The total *smyd* expression level in white muscle was approximately 2- to 3-fold higher than that in red muscle. In both muscle types, *smyd1a* was the predominant paralog, while *smyd1b* represented the secondary contributor; all other *smyd* members were expressed at comparatively low levels. Relative abundance analysis revealed that white muscle displayed a simpler *smyd* expression composition, with *smyd1a* and *smyd1b* collectively accounting for the vast majority of total *smyd* transcripts. By contrast, red muscle exhibited a more complex *smyd* expression profile, with additional contributions from *smyd2b* and *smyd5* (Fig. 8B).

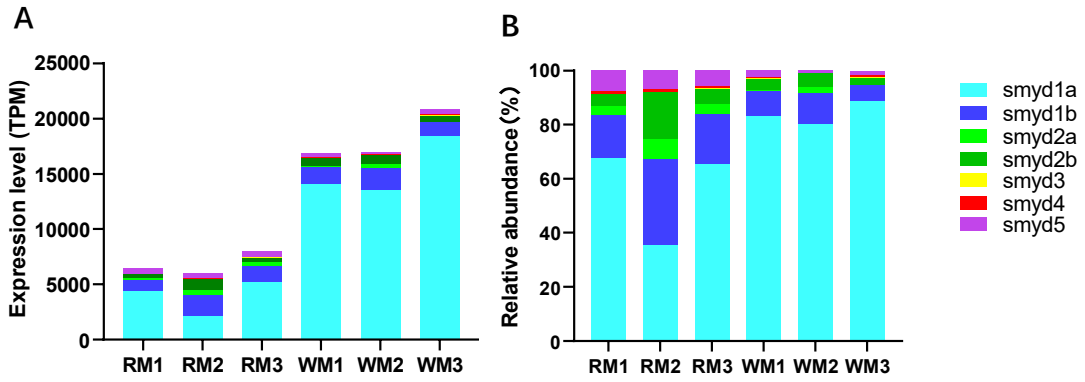


Fig. 8 Comparison of *smyd* genes expression in white and red muscle in Chinese perch. (A) Expression pattern of *smyd* genes in white and red muscle. (B) Relative abundance of *smyd* subtypes in white and red muscle. WM and RM refer to white muscle and red muscle, respectively.

3.10. Histological changes following CTX-induced skeletal muscle injury in Chinese perch

H&E staining revealed relatively intact and compactly organized muscle fibers in the uninjured muscle at 0 dpi. Following CTX injection, marked local disruption of muscle architecture, irregular fiber morphology, and widened inter-fiber spaces were evident at 1 dpi. Pronounced focal structural disruption persisted at 3 dpi. At 5 dpi, the overall tissue architecture showed partial restoration, although localized abnormalities remained. By 7 dpi, gross tissue disruption was reduced and muscle continuity was further restored, while substantial heterogeneity in muscle fiber size and numerous small-diameter fibers were still observed, suggesting ongoing tissue remodeling (Fig. 9).

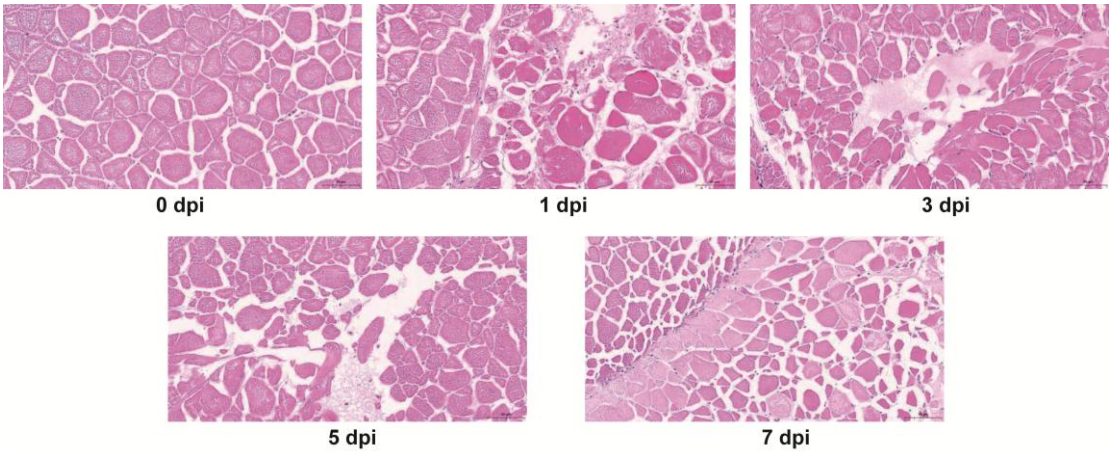


Fig. 9 Histological changes in Chinese perch skeletal muscle following CTX-induced injury. H&E-

stained sections of dorsal white muscle from the uninjured control group (0 dpi) and at 1, 3, 5, and 7 days post-injury (dpi). Scale bar = 50 μm.

3.11. Analysis of *smyd* gene expression after muscle injury in Chinese perch

To investigate the potential involvement of *smyd* genes in skeletal muscle injury responses, the expression levels of seven *smyd* genes were examined in CTX-injured white muscle at 1, 3, 5 and 7 dpi by qPCR. The *smyd* family members displayed distinct temporal expression patterns after muscle injury (Fig. 10). Among them, *smyd1a* showed a different early response pattern compared with the other *smyd* genes. Its expression did not decrease at 1 dpi and was maintained at a level comparable to that of the uninjured control group. Subsequently, *smyd*1a expression increased and reached its highest level at 5 dpi, followed by a decrease at 7 dpi. By contrast, *smyd1b*, *smyd2a*, *smyd2b*, *smyd3* and *smyd4* showed reduced expression at 1 dpi, followed by partial or marked recovery at later time points. *The smyd1b*, *smyd2a*, *smyd2b* and *smyd3* showed prominent induction at 5 dpi. *The smyd4* showed an early decrease followed by recovery toward the basal level. *The smyd5* did not exhibit significant changes among the examined time points.

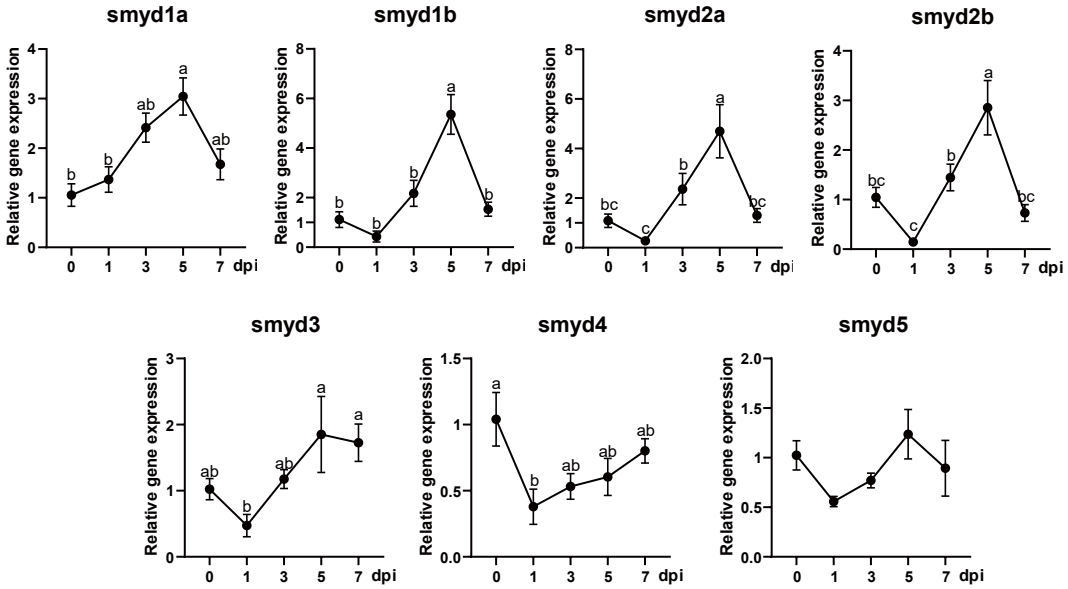


Fig. 10 Temporal expression changes of *smyd* genes after CTX-induced skeletal muscle injury in Chinese perch. Relative expression levels of *smyd* genes were examined in uninjured control muscle and at 1, 3, 5, and 7 days post-injury. The uninjured control group is shown as 0 dpi. Values represent the mean ± SEM. Statistical significance was determined by one-way ANOVA followed by Tukey's multiple comparisons test. Different lowercase letters indicate significant differences among groups at $P < 0.05$.

4. Discussion

The number of *smyd* family members varies across vertebrate lineages. Mammals such as humans and mice typically possess five *smyd* genes, whereas teleost fishes, including zebrafish and Chinese perch, retain *seven* members. This expansion is consistent with the teleost-specific whole-genome duplication event and subsequent differential retention of duplicated genes (Jaillon et al. 2004; Leinhart and Brown 2011). In the present study, seven *smyd* genes were identified in Chinese perch, consistent with this teleost-specific pattern. Structural analyses showed that Chinese perch SMYD proteins retain the core SET-associated architecture typical of this lysine methyltransferase family, while also displaying member-specific divergence. The *smyd1*, *smyd2*, and *smyd3* members shared relatively conserved domain organization, motif composition, and predicted tertiary folds, suggesting preservation of the

catalytic and protein-interaction framework characteristic of SMYD proteins (Rueda-Robles et al. 2021; Padilla et al. 2023). By contrast, *smyd4* and *smyd5* exhibited more divergent structural features. *Smyd4* exhibited a distinct domain organization, with the zf-MYND domain positioned outside the SET domain, whereas the canonical zf-MYND domain was not clearly detected in *smyd5* under the present annotation criteria. This pattern supports the view that *smyd* family members have diversified in structural organization and biological function during evolution (Rueda-Robles et al. 2021; Han et al. 2024). The AlphaFold 3-based predictions were consistent with this interpretation, as SMYD1a/SMYD1b and SMYD2a/SMYD2b showed high structural similarity, whereas SMYD4 and SMYD5 appeared to display more distinct global features in the predicted models. However, because these models are computational predictions, the inferred structure-function relationships require further validation through experimental structural analyses, enzymatic assays, and targeted mutagenesis. The phylogenetic and synteny results further supported the orthology assignment and evolutionary conservation of Chinese perch *smyd* genes. Chinese perch smyd members clustered with their corresponding vertebrate orthologs and were divided into five conserved subfamilies. The duplicated *smyd1a*/*smyd1b* and *smyd2a*/*smyd2b* pairs formed teleost-specific subclades, supporting their origin from teleost genome duplication. Comparative synteny showed that all seven Chinese perch *smyd* loci are conserved in synteny with large yellow croaker. The intact synteny of the *smyd2a/smyd3*-containing region between these two percomorph species suggests that the ancestral chromosomal organization has been maintained in these related teleost lineages. In contrast, the more fragmented syntenic links observed between Chinese perch and zebrafish may reflect lineage-specific chromosomal rearrangements. Notably, the duplicated SMYD1 and SMYD2 paralogs retained similar predicted protein folds but showed distinct developmental and tissue-expression profiles, suggesting that post-duplication divergence in Chinese perch *smyd* genes has occurred mainly through regulatory divergence rather than major protein-structural changes.

The spatiotemporal expression profiles provided important evidence for functional diversification among Chinese perch *smyd* members. During embryonic and early larval development, *smyd1b*, *smyd2a*, and *smyd5* were relatively abundant at early stages, whereas *smyd1a* became more evident from the tail-bud stage onward. This temporal separation suggests that different *smyd* members may participate in distinct developmental phases. The early expression of *smyd1b* is consistent with zebrafish studies showing that *smyd1b* has a prominent embryonic role in myofibrillogenesis, while *smyd1a* plays a weaker role or later during early development (Gao et al. 2014; Cai et al. 2019). In contrast, the later onset and sustained post-hatching expression of *smyd1a*, together with its strong enrichment in adult skeletal muscle, especially white muscle, support a closer association with muscle differentiation, growth, and maintenance. This interpretation agrees with the established role of *smyd1* as a muscle-enriched methyltransferase required for myofibril organization, sarcomere integrity, myosin expression, and muscle function (Tan et al. 2006; Just et al. 2011; Jiao et al. 2021). In mice, loss of SMYD1 selectively impairs fast-twitch muscle fibers, suggesting an important role in glycolytic muscle maintenance (Nagandla et al. 2016). Therefore, the predominance of *smyd1a* in post-hatching and adult white muscle suggests that this paralog is more closely associated with continued fast skeletal muscle growth, contractile structure maintenance, and muscle fiber integrity than with the earliest embryonic myogenic program. The persistence of moderate *smyd1b* expression in muscle also suggests partial functional overlap with smyd1a in specific contexts, although smyd1b appears more embryo-biased (Paone et al. 2018). A similar regulatory divergence was observed between the *smyd2* paralogs. *smyd2a* showed high early expression and broad tissue distribution, consistent with the known pleiotropic roles of *smyd2* in cell proliferation, apoptosis regulation, and histone and non-histone protein methylation (Cho et al. 2012;

Yi et al. 2019). By contrast, *smyd2b* was preferentially expressed in skeletal muscle, myocardium, esophagus, and intestine, suggesting a stronger association with muscle-rich tissues and possible specialization toward muscle-related processes after duplication. In addition to these paralogous pairs, *smyd3* and *smyd2a* showed broadly similar expression across non-muscle tissues, implying potential overlap in general cellular regulation. This is consistent with the known involvement of *smyd3* in transcriptional activation, cell proliferation, tumorigenesis, and antiviral immunity in Chinese perch (Mazur et al. 2014; Rueda-Robles et al. 2021; Shi et al. 2026). *Smyd5* showed pronounced early embryonic expression followed by a decrease, resembling the early developmental expression reported in zebrafish and supporting a possible role in maternal or early embryonic regulatory programs, including hematopoiesis and heterochromatin maintenance (Fujii et al. 2016; Kidder et al. 2017). The broad expression of *smyd4* and *smyd5* in multiple adult tissues, including gonads, further suggests possible roles outside muscle biology, although their specific functions in fish reproduction and other tissues remain to be clarified. The comparison between red and white muscle further supported the muscle-associated expression pattern of *smyd* genes in Chinese perch. *smyd1a* was the predominant paralog in both muscle types, and total *smyd* expression was higher in white muscle than in red muscle. The higher abundance of *smyd1a* in white muscle is consistent with its possible association with fast skeletal muscle growth or maintenance. This interpretation is also in line with previous evidence that SMYD1 is important for fast-twitch fiber maintenance and sarcomere integrity (Nagandla et al. 2016). In contrast, red muscle showed relatively higher contributions from *smyd1b*, *smyd2b*, and *smyd5* compared with white muscle. This difference suggests that the relative contribution of individual *smyd* members may vary between muscle fiber types, but the functional significance of this pattern requires further investigation.

The injury-response analysis extended these developmental and tissue-expression patterns to adult skeletal muscle repair. Skeletal muscle regeneration after acute injury involves an ordered sequence of myofiber degeneration, inflammatory infiltration, activation and proliferation of muscle stem/progenitor cells, myogenic differentiation, myofibril reassembly, and tissue remodeling. In cardiotoxin-induced injury models, early stages are dominated by degeneration and inflammatory responses, whereas later stages show stronger anabolic signaling, myogenic differentiation, and fiber remodeling (Dalle et al. 2020; Wang et al. 2022). In adult zebrafish, Pax3/Pax7-positive satellite-like cells contribute to repair, and the myogenic response peaks around 4-5 days post-injury (Berberoglu et al. 2017). Histological examination confirmed that CTX injection induced pronounced localized structural damage in the dorsal white muscle of Chinese perch, supporting the validity of the injury model used for subsequent gene-expression analysis. In this context, *smyd1a* showed the most distinctive response among the seven genes. Its expression was maintained at 1 dpi rather than decreasing with most other *smyd* members, and it was subsequently induced at 5 dpi. Given its strong basal enrichment in adult white muscle, the maintenance of *smyd1a* at the early injury stage may reflect preservation of muscle identity or residual myofibrillar maintenance rather than immediate activation of regeneration. Its induction at 5 dpi is more consistent with a role in myogenic differentiation, sarcomere reassembly, and myofiber reconstruction. This interpretation is supported by studies showing that smyd1 is required for myofibril organization, myosin expression, and sarcomere assembly (Tan et al. 2006; Jiao et al. 2021), and by recent evidence that *smyd1* regulates myogenesis through methylation of skNAC and promotes thick filament assembly and sarcomere homeostasis through methylation of sarcomeric myosin heavy chain (Zhu et al. 2023; Diofano et al. 2025). *Smyd1b* also responded dynamically, but its early decrease followed by later induction suggests a more transient suppression during the degenerative/inflammatory phase and reactivation

during remodeling. This difference between *smyd1a* and *smyd1b* is consistent with their divergent developmental profiles and with zebrafish studies showing overlapping but unequal roles of the two paralogs in myofibrillogenesis (Gao et al. 2014; Cai et al. 2019; Paone et al. 2018). The *smyd2* paralogs were also downregulated at 1 dpi and induced later, especially around 5 dpi, suggesting an association with reconstruction of muscle structure rather than with the immediate inflammatory response. Mechanistically, this is plausible because *smyd2* regulates cytoplasmic lysine methylation of Hsp90 and contributes to formation of the *smyd2*-Hsp90-titin complex, thereby supporting titin stability and myofilament organization (Donlin et al. 2012). The later induction of *smyd2a* and *smyd2b* may therefore reflect roles in sarcomere stabilization and recovery of contractile integrity after injury. *Smyd3* showed a more moderate injury response, with early suppression followed by recovery or induction, suggesting possible involvement in the transition from injury response to myogenic differentiation rather than a primary role in acute damage signaling. Previous work has implicated *smyd3* in skeletal muscle differentiation in vitro and in heart and skeletal muscle development in zebrafish (Fujii et al. 2011; Codato et al. 2019), but its relatively low muscle-biased expression in Chinese perch indicates that its role in adult white muscle repair requires further study. Compared with *smyd1*, *smyd2*, and *smyd3*, *smyd4* and *smyd5* showed limited transcriptional responses: smyd4 decreased early and recovered toward the basal level, whereas *smyd5* did not change significantly. Thus, smyd4 and smyd5 showed weaker transcriptional responses during Chinese perch skeletal muscle repair under the present experimental conditions. Overall, the injury data suggest that *smyd1a* is the most relevant candidate for adult white muscle maintenance and repair, while *smyd1b*, *smyd2a*, *smyd2b*, and *smyd3* may contribute to later remodeling or differentiation-related processes. These interpretations are based on mRNA expression patterns, and future protein-level, cell-type-specific, and functional analyses will be needed to establish their direct mechanistic roles.

5. Conclusion

In this study, seven *smyd* gene family members were identified from the genome of Chinese perch (*Siniperca chuatsi*) and classified into five conserved subfamilies (*smyd1, smyd2, smyd3, smyd4,* and *smyd5*) through phylogenetic analysis. Structural characterization revealed a conservation–divergence pattern: *smyd1, smyd2,* and *smyd3* exhibited relatively conserved domain architectures and motif compositions, whereas *smyd4* and *smyd5* showed greater structural divergence, suggesting potential functional specialization during teleost evolution. Expression profiling revealed highly differentiated spatiotemporal patterns across 17 adult tissues and 15 developmental stages. Among the duplicated *smyd1* paralogs, *smyd1b* was relatively enriched during early embryogenesis, whereas *smyd1a* became the dominant paralog in post-hatching and adult white muscle, indicating regulatory divergence between early developmental and adult muscle-associated expression programs. These patterns suggest developmental-stage-specific roles among *smyd* members and regulatory divergence between duplicated *smyd1* and *smyd2* paralogs. In the cardiotoxin-induced skeletal muscle injury model, *smyd* genes exhibited different temporal responses. *The smyd1a* maintained its expression during the early injury stage and was markedly induced at 5 days post-injury, suggesting that it may be associated with adult white muscle maintenance and injury-induced repair. *The smyd1b*, *smyd2a*, *smyd2b*, and *smyd3* also showed later recovery or induction, whereas *smyd4* showed limited recovery and *smyd5* displayed no significant transcriptional change under the present experimental conditions. Collectively, this study provides a comprehensive characterization of the *smyd* gene family in Chinese perch and identifies *smyd1a* as a candidate gene associated with adult skeletal muscle maintenance and repair. However, the present conclusions are mainly based on sequence characterization and mRNA expression patterns.

Further functional studies, including gene knockdown or knockout, protein-level validation, enzymatic activity assays, and cell-type-specific localization analyses, are required to clarify the precise roles and mechanisms of *smyd* genes during skeletal muscle growth and regeneration.

Authorship contribution statement

Conceptualization: Yaxiong Pan, Wuying Chu; Methodology: Dezhi Wu, Yifan Zhu, Shuangli He; Formal analysis and investigation: Yaxiong Pan, Dezhi Wu, Yifan Zhu, Shuangli He, Danshi Bingma, Jinyang Jiang, Linxuan Zhang, Xin Zhu; Data curation: Yaxiong Pan, Dezhi Wu; Validation: Shuangli He, Jinyang Jiang; Visualization: Yaxiong Pan, Dezhi Wu; Writing - original draft preparation: Yaxiong Pan; Writing - review and editing: Zhi Luo, Jianshe Zhang, Wuying Chu; Funding acquisition: Zhi Luo, Wuying Chu; Resources: Zhi Luo; Supervision: Zhi Luo, Wuying Chu; Project administration: Zhi Luo, Wuying Chu.

Declaration of competing interest

The authors declare that they have no known competing financial interests or personal relationships that could have appeared to influence the work reported in this paper.

Funding

This work was supported by the National Key Research and Development Program of China [grant numbers 2024YFD2402000, 2022YFD2400800].

Data availability

The transcriptome datasets analysed in this study are publicly available in the NCBI Sequence Read Archive under BioProject accessions PRJNA496427 (adult tissues and developmental stages) and PRJNA685101 (white and red skeletal muscle). The Chinese perch genome assembly and annotation files are available from the Chinese perch genome portal (http://genomes.igb-berlin.de/Siniperca/). The other data generated in this study are available from the corresponding author upon reasonable request.

References

Abramson J, Adler J, Dunger J, Evans R, Green T, Pritzel A, Ronneberger O, Willmore L (2024) Accurate structure prediction of biomolecular interactions with AlphaFold 3. Nature 630:493-500. https://doi.org/10.1038/s41586-024-07487-w

Bailey TL, Johnson J, Grant CE, Noble WS (2015) The MEME Suite. Nucleic Acids Res 43: W39-W49. https://doi.org/10.1093/nar/gkv416

Berberoglu MA, Gallagher TL, Morrow ZT, Talbot JC, Hromowyk KJ, Tenente IM, Langenau DM, Amacher SL (2017) Satellite-like cells contribute to Pax7-dependent skeletal muscle repair in adult zebrafish. Dev Biol 424:162-180. https://doi.org/10.1016/j.ydbio.2017.03.004

Bottino C, Peserico A, Simone C, Caretti G (2020) SMYD3: an oncogenic driver targeting epigenetic regulation and signaling pathways. Cancers 12:142. https://doi.org/10.3390/cancers12010142

Cai M, Han L, Liu L, He F, Chu W, Zhang J, Tian Z, Du S (2019) Defective sarcomere assembly in smyd1a and smyd1b zebrafish mutants. FASEB J 33:6209-6225. https://doi.org/10.1096/fj.201801578R

Chen C, Chen H, Zhang Y, Thomas HR, Frank MH, He Y, Xia R (2020) TBtools: an integrative toolkit developed for interactive analyses of big biological data. Mol Plant 13:1194-1202. https://doi.org/10.1016/j.molp.2020.06.009

Chen L, Pan Y, Cheng J, Zhu X, Chu W, Meng YY, Bin S, Zhang J (2023) Characterization of myosin heavy chain (MYH) genes and their differential expression in white and red muscles of Chinese perch, Siniperca chuatsi. Int J Biol Macromol 250:125907. https://doi.org

/10.1016/j.ijbiomac.2023.125907
Cho HS, Shimazu T, Toyokawa G, Daigo Y, Maehara Y, Hayami S, Ito A, Masuda K, Ikawa N, Field HI, Tsuchiya E, Ohnuma S, Ponder BAJ, Yoshida M, Nakamura Y, Hamamoto R (2012) Enhanced HSP70 lysine methylation promotes proliferation of cancer cells through activation of Aurora kinase B. Nat Commun 3:1072. https://doi.org/10.1038/ncomms2074
Chu W, Fu G, Chen J, Chen D, Meng T, Zhou R, Xia X, Zhang J (2010) Gene expression profiling in muscle tissues of the commercially important teleost, Siniperca chuatsi L. Aquac Int 18:667-678. https://doi.org/10.1007/s10499-009-9289-8
Chu W, Zhang F, Song R, Li Y, Wu P, Chen L, Cheng J, Du SJ, Zhang J (2017) Proteomic and microRNA transcriptome analysis revealed the microRNA-SmyD1 network regulation in skeletal muscle fibers performance of Chinese perch. Sci Rep 7:16498. https://doi.org/10.1038/s41598-017-16718-2
Codato R, Perichon M, Divol A, Fung E, Sotiropoulos A, Bigot A, Weitzman JB, Medjkane S (2019) The SMYD3 methyltransferase promotes myogenesis by activating the myogenin regulatory network. Sci Rep 9:17298. https://doi.org/10.1038/s41598-019-53577-5
Dalle S, Hiroux C, Poffé C, Ramaekers M, Wouters S, Deldicque L, Koppo K (2020) Cardiotoxin-induced skeletal muscle injury elicits profound changes in anabolic and stress signaling, and muscle fiber type composition. J Muscle Res Cell Motil 41:375-387. https://doi.org/10.1007/s10974-020-09584-5
Diofano F, Amadi C, Hartmann L, Gahr BM, Weinmann-Emhardt K, Rottbauer W, Just S (2025) SMYD1-mediated mono-methylation of lysine K35 of sarcomeric myosin heavy chain (MHC) regulates sarcomere assembly and homeostasis in zebrafish and human iPSC-derived cardiomyocytes. J Mol Cell Cardiol 208:74-84. https://doi.org/10.1016/j.yjmcc.2025.09.002
Donlin LT, Andresen C, Just S, Rudensky E, Pappas CT, Kruger M, Jacobs EY, Unger A, Zieseniss A, Dobenecker MW, Voelkel T, Chait BT, Gregorio CC, Rottbauer W, Tarakhovsky A, Linke WA (2012) Smyd2 controls cytoplasmic lysine methylation of Hsp90 and myofilament organization. Genes Dev 26:114-119. https://doi.org/10.1101/gad.177758.111
Du SJ, Tan X, Zhang J (2014) SMYD proteins: key regulators in skeletal and cardiac muscle development and function. Anat Rec 297:1650-1662. https://doi.org/10.1002/ar.22972
Fujii T, Tsunesumi S, Yamaguchi K, Watanabe S, Furukawa Y (2011) Smyd3 is required for the development of cardiac and skeletal muscle in zebrafish. PLoS One 6:e23491. https://doi.org/10.1371/journal.pone.0023491
Fujii T, Tsunesumi S, Sagara H, Munakata M, Hisaki Y, Sekiya T, Furukawa Y, Sakamoto K, Watanabe S (2016) Smyd5 plays pivotal roles in both primitive and definitive hematopoiesis during zebrafish embryogenesis. Sci Rep 6:29157. https://doi.org/10.1038/srep29157
Gao J, Li J, Li BJ, Yagil E, Zhang J, Du SJ (2014) Expression and functional characterization of smyd1a in myofibril organization of skeletal muscles. PLoS One 9:e86808. https://doi.org/10.1371/journal.pone.0086808
Glasauer SMK, Neuhauss SCF (2014) Whole-genome duplication in teleost fishes and its evolutionary consequences. Mol Genet Genomics 289:1045-1060. https://doi.org/10.1007/s00438-014-0889-2
Han TS, Kim DS, Son MY, Cho HS (2024) SMYD family in cancer: epigenetic regulation and molecular mechanisms of cancer proliferation, metastasis, and drug resistance. Exp Mol Med 56:2325-2336. https://doi.org/10.1038/s12276-024-01326-8

Hardy D, Besnard A, Latil M, Jouvion G, Briand D, Thépenier C, Pascal Q, Guguin A, Gayra ud-Morel B, Cavaillon JM, Tajbakhsh S, Rocheteau P, Chrétien F (2016) Comparative stud y of injury models for studying muscle regeneration in mice. PLoS One 11:e0147198. http s://doi.org/10.1371/journal.pone.0147198

He S, Li L, Lv LY, Cai WJ, Dou YQ, Li J, Tang SL, Chen X, Zhang Z, Xu J, Zhang YP, Yin Z, Wuertz S, Tao YX, Kuhl H, Liang XF (2020) Mandarin fish (Sinipercidae) genom es provide insights into innate predatory feeding. Commun Biol 3:361. https://doi.org/10.10 38/s42003-020-1094-y

Hwang I, Gottlieb PD (1995) Bop: a new T-cell-restricted gene located upstream of and opposi te to mouse CD8b. Immunogenetics 42:353-361. https://doi.org/10.1007/BF00179396

Hwang I, Gottlieb PD (1997) The Bop gene adjacent to the mouse CD8b gene encodes distinc t zinc-finger proteins expressed in CTLs and in muscle. J Immunol 158:1165-1174. https:// doi.org/10.4049/jimmunol.158.3.1165

Jaillon O, Aury JM, Brunet F, et al (2004) Genome duplication in the teleost fish Tetraodon n igroviridis reveals the early vertebrate proto-karyotype. Nature 431:946-957. https://doi.org/1 0.1038/nature03025

Jiao S, Xu R, Du S (2021) Smyd1 is essential for myosin expression and sarcomere organizati on in craniofacial, extraocular, and cardiac muscles. J Genet Genomics 48:208-218. https:// doi.org/10.1016/j.jgg.2021.03.004

Johnston IA, Bower NI, Macqueen DJ (2011) Growth and the regulation of myotomal muscle mass in teleost fish. J Exp Biol 214:1617-1628. https://doi.org/10.1242/jeb.038620

Just S, Meder B, Berger IM, et al (2011) The myosin-interacting protein SMYD1 is essential f or sarcomere organization. J Cell Sci 124:3127-3136. https://doi.org/10.1242/jcs.084772

Kidder BL, He R, Wangsa D, Padilla-Nash HM, Bernardo MM, Sheng S, Ried T, Zhao K (20 17) SMYD5 controls heterochromatin and chromosome integrity during embryonic stem cel l differentiation. Cancer Res 77:6729-6745. https://doi.org/10.1158/0008-5472.CAN-17-0828

Leinhart K, Brown M (2011) SET/MYND lysine methyltransferases regulate gene transcription and protein activity. Genes 2:210-218. https://doi.org/10.3390/genes2010210

Letunic I, Bork P (2021) Interactive Tree Of Life (iTOL) v5: an online tool for phylogenetic t ree display and annotation. Nucleic Acids Res 49:W293-W296. https://doi.org/10.1093/nar/g kab301

Li X, Zhang J (2009) Structure and function of zinc finger proteins in eukaryotes. Chin J Bio chem Mol Biol 25:206-212. https://doi.org/10.13865/j.cnki.cjbmb.2009.03.016

Mazur PK, Reynoird N, Khatri P, et al (2014) SMYD3 links lysine methylation of MAP3K2 t o Ras-driven cancer. Nature 510:283-287. https://doi.org/10.1038/nature13320

Meng Y, Zeng W, Zhu X, et al (2025) The role of Twist2 in myoblast proliferation, fusion, a nd its impact on muscle structure during the growth of Chinese perch (Siniperca chuatsi). Animals 15:1177. https://doi.org/10.3390/ani15081177

Nagandla H, Lopez S, Yu W, Rasmussen TL, Tucker HO, Schwartz RJ, Stewart MD (2016) D efective myogenesis in the absence of the muscle-specific lysine methyltransferase SMYD1. Dev Biol 410:86-97. https://doi.org/10.1016/j.ydbio.2015.12.005

Nemova NN, Kantserova NP, Lysenko LA (2021) The traits of protein metabolism in the skele tal muscle of teleost fish. J Evol Biochem Physiol 57:626-645. https://doi.org/10.1134/S002 2093021030121

Padilla A, Manganaro JF, Huesgen L, et al (2023) Targeting epigenetic changes mediated by members of the SMYD family of lysine methyltransferases. Molecules 28:2000. https://doi.org/10.3390/molecules28042000

Paone C, Rudeck S, Etard C, Strähle U, Rottbauer W, Just S (2018) Loss of zebrafish smyd1a interferes with myofibrillar integrity without triggering the misfolded myosin response. Biochem Biophys Res Commun 496:339-345. https://doi.org/10.1016/j.bbrc.2018.01.060

Rossi GS, Borowiec BG (2024) Fish muscle physiology and plasticity. In: Alderman SL, Gillis TE (eds) Encyclopedia of fish physiology, 2nd edn. Academic Press, Amsterdam, pp 519-528. https://doi.org/10.1016/B978-0-323-90801-6.00025-2

Rueda-Robles A, Audano M, Álvarez-Mercado AI, Rubio-Tomás T (2021) Functions of SMYD proteins in biological processes: what do we know? An updated review. Arch Biochem Biophys 712:109040. https://doi.org/10.1016/j.abb.2021.109040

Schrödinger LLC (2015) The PyMOL Molecular Graphics System, Version 1.7.2.1. Schrödinger LLC, New York

Shen Y, Cao M, Tang S, Zhao Y, Zhao J, Chen X, Bi Y (2020) Genomic and functional characterization of the lect2 gene from Siniperca chuatsi. Fish Shellfish Immunol 107:146-155. https://doi.org/10.1016/j.fsi.2020.09.034

Shi S, Wang Z, Xiao W, et al (2026) Molecular characteristics and functions of the SMYD3 gene in antiviral immunity in Siniperca chuatsi. Acta Hydrobiol Sin 50:042615. https://doi.org/10.3724/1000-3207.2025.2025.0373

Tamura K, Stecher G, Kumar S (2021) MEGA11: Molecular Evolutionary Genetics Analysis Version 11. Mol Biol Evol 38:3022-3027. https://doi.org/10.1093/molbev/msab120

Tan X, Rotllant J, Li H, De Deyne P, Du SJ (2006) SmyD1, a histone methyltransferase, is required for myofibril organization and muscle contraction in zebrafish embryos. Proc Natl Acad Sci U S A 103:2713-2718. https://doi.org/10.1073/pnas.0509503103

Wang K, Zhu X, Li Y, Chen D, Wu P, Chu W (2016) Molecular characterization and expression regulation of smyd1a and smyd1b in skeletal muscle of Chinese perch (Siniperca chuatsi). Comp Biochem Physiol B Biochem Mol Biol 194:25-31. https://doi.org/10.1016/j.cbpb.2016.01.004

Wang Y, Lu J, Liu Y (2022) Skeletal muscle regeneration in cardiotoxin-induced muscle injury models. Int J Mol Sci 23:13380. https://doi.org/10.3390/ijms232113380

Wu L, Kou F, Ji Z, Li B, Zhang B, Guo Y, Yang L (2021a) SMYD2 promotes tumorigenesis and metastasis of lung adenocarcinoma through RPS7. Cell Death Dis 12:439. https://doi.org/10.1038/s41419-021-03720-w

Wu P, Chen L, Cheng J, Pan Y, Zhu X, Bao L, Chu W, Zhang J (2021b) The miRNA expression profile directly reflects the energy metabolic differences between slow and fast muscle with nutritional regulation of the Chinese perch Siniperca chuatsi. Comp Biochem Physiol A Mol Integr Physiol 259:111003. https://doi.org/10.1016/j.cbpa.2021.111003

Xiao D, Wang H, Hao L (2018) The roles of SMYD4 in epigenetic regulation of cardiac development in zebrafish. PLoS Genet 14:e1007578. https://doi.org/10.1371/journal.pgen.1007578

Xie J, Chen Y, Cai G, Cai R, Hu Z, Wang H (2023) Tree Visualization By One Table (tvBOT): a web application for visualizing, modifying and annotating phylogenetic trees. Nucleic Acids Res 51:W587-W592. https://doi.org/10.1093/nar/gkad359

Yi X, Jiang XJ, Fang ZM (2019) Histone methyltransferase SMYD2: ubiquitous regulator of di

sease. Clin Epigenetics 11:112. https://doi.org/10.1186/s13148-019-0711-4
Zhu L, Brown MA, Sims RJ, Tiwari GR, Nie H, Mayfield RD, Tucker HO (2023) Lysine methyltransferase SMYD1 regulates myogenesis via skNAC methylation. Cells 12:1695. https://doi.org/10.3390/cells12131695